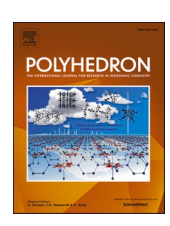


Contents lists available at ScienceDirect

# Polyhedron

journal homepage: www.elsevier.com/locate/poly





# DFT study of electrostatic effects upon methane activation by early, high-valent multiply bonded complexes

Sarah Ann Teaw, Thomas R. Cundari

Contribution from The Department of Chemistry, Center for Advanced Scientific Computing and Modeling (CASCaM), The University of North Texas, Denton, TX 762034. United States

#### ARTICLE INFO

Keywords: Vanadium Methane activation DFT Electrostatic effects

#### ABSTRACT

The research presented here focuses on the electrostatic effect of varying alkali metal cations (Li<sup>+</sup> through Cs<sup>+</sup>) in the outer coordination sphere of model methane activating complexes with metal-nitrogen multiple bonds. Lighter metal alkali metal cations yield reduced methane activation barriers ( $\Delta G^{\dagger}$ ), with the lowest barrier computed for the Li<sup>+</sup> salt; moreover, all modeled salts have lower  $\Delta G^{\dagger}$  than the corresponding anion in polar solvents. Via variation of the polarity of continuum solvents, this research also indicates that electrostatic effects are likely to be manifested most significantly in the low polarity, hydrophobic solvents typically used for inorganic and organometallic complexes capable of methane activation. Taken together, the results of these DFT simulations suggest that electrostatic effects have the potential to significantly decrease methane activation barriers.

#### 1. Introduction

The global warming potential of methane is greater than that of carbon dioxide by a factor of 25 [1]. Catalytic methane activation and functionalization has the potential to convert methane gas to liquid methanol, decreasing the need to "flare" methane (which releases CO<sub>2</sub>) and increasing supplies of methanol, a valuable chemical. However, because methane does not react readily, and when it does react it is typically under forcing conditions, finding active and selective catalysts for methane conversion remains a crucial need.

Olah et al. showed that methane activation is possible when employing largely main group-based superacids [2]. Exploiting very strong acid/base interactions in d-block chemistry, Wolczanski and coworkers [3] showed in pioneering research that highly Lewis acidic d<sup>0</sup>-transition metal ions coupled with highly basic imide actor ligands could readily activate methane via 1,2-C—H addition to metal-nitrogen multiple bonds. Recent DFT studies also implicate 1,2-C—H addition as the preferred pathway for methane C—H activation by early, high-valent transition metal nitride complexes [4–6].

Inorganic and organometallic catalysis has traditionally focused on modifying the metal–ligand active site by manipulating the metal, actor ligand, supporting ligands and/or ligand substituents. As such chemists have emphasized changes to the metal's inner coordination sphere.

Recent research, however, has begun to explore outer coordination sphere effects – dispersion, nucleophiles, electrostatics – in the search for more active and selective catalysts [7–9], albeit less so for unadorned substrates like light alkanes. For example, Wolczanski and co-workers demonstrated that dispersion effects played a significant role in rates of migratory insertion involving iron-imide complexes [8]. In other research, our team showed that outer-coordination sphere nucleophiles substantially lower methane activation barriers by up to 10 kcal/mol via kinetic (transition state stabilization) means as opposed to simply increasing the thermodynamic driving force [7].

The chemical bonding properties of metal-nitride complexes have been found to be greatly affected by their coordination environment [10,11]. Vanadium nitride complexes activate methane via 1,2-C—H addition to their metal-nitrogen multiple bonds [4,5], a mechanism akin to that which has been deduced for the  $d^0$  Wolczanski systems [3]. Experiments and DFT simulations have unraveled an interesting radical process for conversion of methane to acetic acid mediated by  $V^V$ -oxoperoxo complexes [12]. Deng et al. have reported several  $d^0$  systems, including  $V^V$ , which can functionalize methane under electrocatalytic conditions that generate highly reactive O-based radicals capable of cleaving the strong C—H bond of methane [13,14].

Experiments by Yang and coworkers [9] suggest that outer sphere electrostatic effects may impact the chemistry of manganese nitrides.

<sup>\*</sup> Corresponding author.

E-mail address: %20t@unt.edu (T.R. Cundari).

Calculations by Najafian and Cundari [15] indicate that outer sphere s-block metal ions appended to supporting ligand functionalities can also lower activation barriers for methane activation by middle-series MnN complexes. Considering these and other literature precedents [16], we thus sought to investigate whether methane activation barriers for more prevalent high valent, early d-block nitrides could be modulated via electrostatic effects engendered by alkali metal cations.

#### 2. Computational methods

Using the Gaussian16 package [17], density functional theory was utilized to optimize all geometries; free energies assume standard temperature (298.15 K) and pressure (1 atm) for gas-phase simulations. The compounds were optimized using the B3LYP functional and def2-TZVPP basis set; all alkali metal species were predicted to be ground state singlets. The enthalpies and Gibbs free energies were calculated, as well as vibrational frequencies, to account for the appropriate number of imaginary frequencies for ground and transition state structures. The SMD continuum solvent model [18] was used to assess solvent environments of varying polarity, including benzene, THF, acetone, acetonitrile, and water; methane activation was also studied in the absence of a solvent (gas phase).

#### 3. Results and discussion

#### 3.1. Geometries

The Gibbs free energies, enthalpies, atomic charges, bond lengths,

and bond angles of reactant, product and transition state stationary points were analyzed for each  $VN^-/A^+$  complex interacting with methane. The model activating complex is composed of  $V^{5+}$  central metal ion, a nitride actor ligand, hydroxyl supporting ligands, Fig. 1. An alkali cation  $(A^+)$  is then ligated to the hydroxyl supporting ligands and thus placed in the outer coordination sphere relative to the metal-nitride active site. The reaction between the  $VN^-/A^+$  complex and methane  $(CH_4)$  via the expected 1,2-C—H addition transition state [3–6] yields a product with a new V-methyl bond with concomitant conversion of the nitride ligand to an imide (NH), Fig. 2.

Optimized geometries of the alkali metal/vanadium nitride stationary points show the expected correlations between the size of the alkali metal ions and the length of the bonds they make to the ligating oxygen atoms. The VN bond lengths increase slightly as a function of the alkali metal cation, Figs. 1–3. In the nitride reactants, for example, optimized V≡N bond lengths increase slightly from 1.539 to 1.545 Å for the Li<sup>+</sup> to the Cs<sup>+</sup> salt, respectively, Fig. 1. Calculated bond lengths for transition states (TSs) and products deviate very slightly from these trends; for example, optimized V\(\exists N\) transition state bond lengths are 1.596, 1.604, 1.603, 1.604, and 1.604 Å for Li<sup>+</sup>, Na<sup>+</sup>, K<sup>+</sup>, Rb<sup>+</sup>, and Cs<sup>+</sup>, respectively, Fig. 2. Note, that the bond length of the vanadium-nitrogen is lengthened (by  $\sim$ 4 %) in the TS relative to the reactant nitrides. In the imide product, bond lengths decrease and then increase, although again the differences are very small: 1.646, 1.644, 1.659, 1.649, 1.649 Å for Li<sup>+</sup>, Na<sup>+</sup>, K<sup>+</sup>, Rb<sup>+</sup>, and Cs<sup>+</sup> salts, respectively (Fig. 3). Similar trends are reflected in the two V—O bonds that ligate the alkali metal cation, i.e., bond lengths decrease as the alkali metal increases in size for both reactant and product states, Fig. 1 and Fig. 3. The transition states again

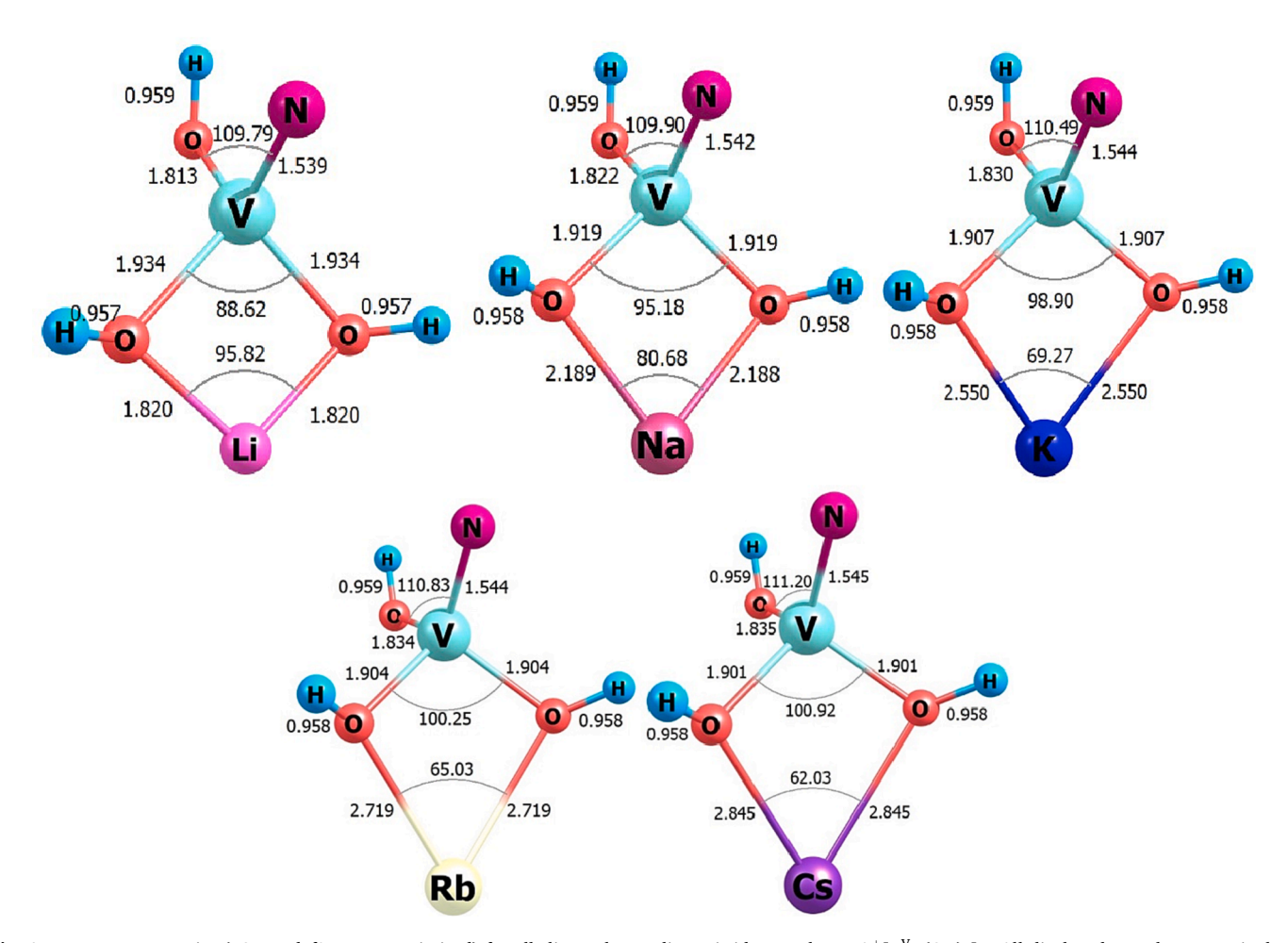


Fig. 1. Reactant geometries (B3LYP/def2-TZVPP optimized) for alkali metal/vanadium nitride complexes,  $A^+[V^VN(OH)_3]^-$ . All displayed complexes are singlets. Bond angles in degrees; bond lengths in Angstrom units.

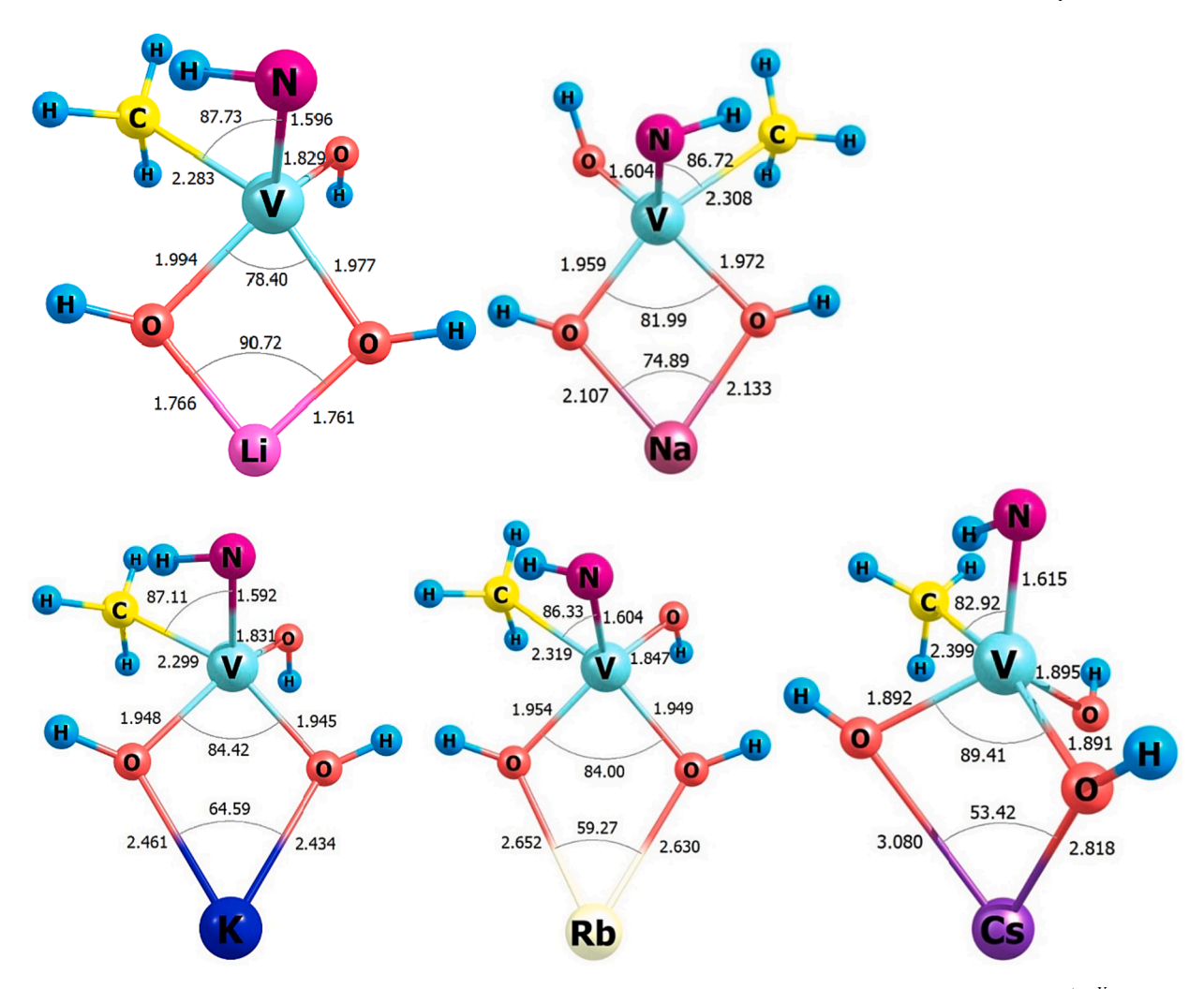


Fig. 2. Transition state geometries (B3LYP/def2-TZVPP optimized) for 1,2-C—H addition to alkali metal/vanadium nitride complexes,  $A^+[V^VN(OH)_3]^-$ . All displayed complexes are singlets. Bond angles in degrees; bond lengths in Angstrom units.

deviate from this metric trend, as the V—O bond length of the compounds in the transition state calculations were 1.977, 1.972, 1.960, 1.954, 1.895 Å for Li<sup>+</sup>, Na<sup>+</sup>, K<sup>+</sup>, Rb<sup>+</sup>, and Cs<sup>+</sup> complexes, respectively. Importantly, alterations to the core geometry of the anionic V $\equiv$ N complexes by varying the alkali metal counterion are very small, Table 1, implying that the computed changes in energetics discussed below more fully reflect underlying variations in electronic structure rather than geometric perturbations.

# 3.2. Impact of outer coordination sphere alkali metals upon C—H activation barriers

From the data in Table 1, the calculated sample standard deviations for the calculated enthalpies and free energies of activation are both  $\sim\pm3\%$  kcal/mol for the range of cations studied. The values calculated for five alkali metal salts studied herein thus closely mirror the standard deviation of enthalpies in a prior study of the impact of outer coordination sphere nucleophiles upon methane activation [7], ca.  $\pm3.5$  kcal/mol. The DFT calculations thus reveal that electrostatic effects significantly modulate methane activation barriers.

## 3.3. Correlations among alkali metal ions

#### 3.3.1. Hammond Postulate

Table 1 collects the calculated free energy barriers and reaction free energies for methane activation for each alkali metal cation in the  $A^+/$ 

VN model complexes. The presence of a heavier alkali metal in the outer coordination sphere results in higher Gibbs free energy barriers for methane activation, Table 1. While the computed methane activation barriers are large, as expected for a reaction involving the strong triple bond of a  $d^0\text{-V}^\text{V}\text{N}$  complex, what is of greater interest in the present context is that  $\Delta G^\ddagger$  can be reduced by the choice of outer sphere cation. Lighter alkali metals present lower methane activation barriers, e.g., the Li $^+$  salt has a lower barrier of  $\sim\!52$  kcal/mol, and reaction energies somewhat closer to thermoneutral, Table 1. An anionic vanadium nitride anion (i.e., alkali metal absent) was simulated for methane activation in acetonitrile and water. These calculations show that alkali metal ions appended systems have lower energy methane activation barriers than does the parent anionic nitride complex (vide infra).

Among the alkali metal ions analyzed (Li $^+$ , Na $^+$ , K $^+$ , Rb $^+$ , Cs $^+$ ), the Gibbs free energies of activation and reaction display a linear trend with a modest positive correlation, R $^2$  ~0.78, Fig. 4, thus conforming to Hammond's Postulate [19]. Hence, unlike previous studies on methane activation in the presence of outer-sphere nucleophiles [7], electrostatic effects seem to arise from both kinetic and thermodynamic origins. To this end, correlations with calculated electronic structure properties of the A $^+$ [V $^V$ N(OH) $_3$ ] $^-$  were investigated.

#### 3.3.2. Electrostatic effects of alkali metal ions

To assess the impact of electrostatics, calculated Mulliken charges for active site atoms of the reactant nitride complexes are tabulated and correlations with calculated activation barriers sought. In the present

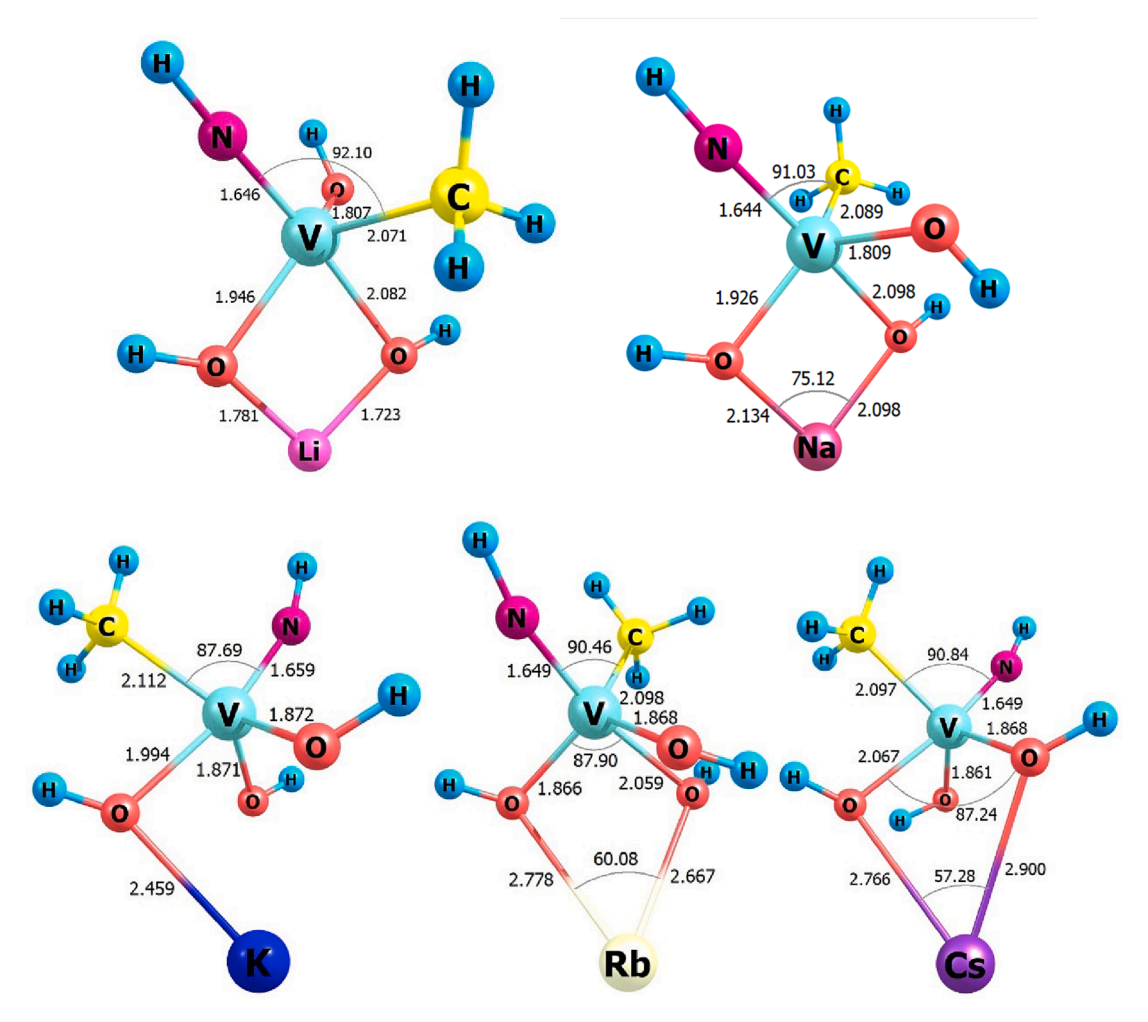
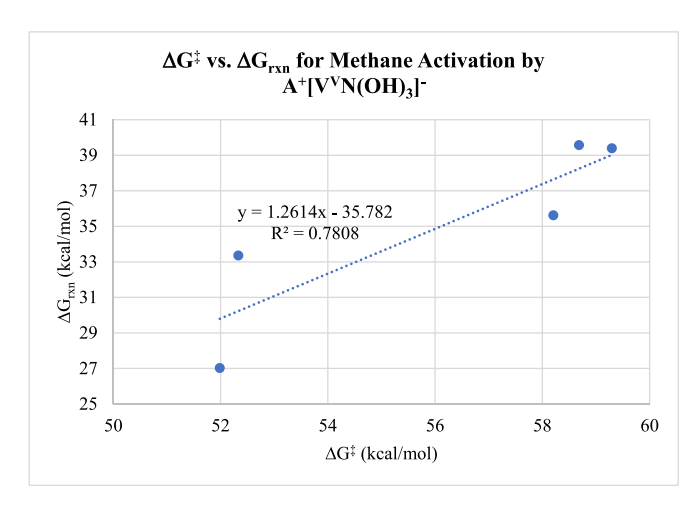


Fig. 3. Product geometries (B3LYP/def2-TZVPP optimized) generated by 1,2-C—H addition of methane to alkali metal/vanadium nitride reactants,  $A^+[V^NN(OH)_3]^-$ . All displayed complexes are singlets. Bond angles in degrees; bond lengths in Angstrom units.

 $\label{thm:calculated} \begin{tabular}{ll} \textbf{Table 1} \\ \textbf{Calculated enthalpy and Gibbs free energy barriers (kcal/mol) for methane activation via 1,2-C—H addition of methane to the V-nitrogen triple bond of $A^{+}[VN(OH)_{3}]^{-}$. \end{tabular}$ 

	Activation Barrier		Reaction Energy	
$A^+$	Enthalpy ΔH <sup>‡</sup> (kcal/mol)	Free Energy $\Delta G^{\ddagger}$ (kcal/mol)	Enthalpy ΔH (kcal/mol)	Free Energy ΔG (kcal/mol)
Li <sup>+</sup>	40.5	52.0	16.5	27.0
Na <sup>+</sup>	41.0	52.3	22.5	33.4
K <sup>+</sup>	46.5	58.2	24.0	35.6
$Rb^+$	47.5	59.3	27.8	39.4
Cs <sup>+</sup>	47.1	58.7	28.1	39.6
Average	44.6	56.1	23.8	35.0
Standard Deviation	$\pm 3.5$	±3.6	±4.7	$\pm 5.2$

research, comparisons are made among highly related chemical entities, so that changes in computed atomic charges are expected to be reasonable. The nitride nitrogen Mulliken atomic charge, Fig. 5, shows the greatest correlation with the free energy barrier of methane activation among the atomic charges investigated, Fig. 5,  $\rm R^2\sim0.85$ , a much stronger correlation than for vanadium atomic charge/energy barrier ( $\rm R^2\sim0.019$ ) and alkali metal/energy barrier charge ( $\rm R^2\sim0.55$ ). The correlation in Fig. 5 indicates that a less negative (i.e., more electrophilic/less basic) nitride – arising from a less electropositive alkali metal in the outer coordination sphere – yields lower energy barriers and thus



**Fig. 4.** Calculated free energy barriers of activation (x-axis) versus reaction free energies (y-axis) for methane activation by alkali metal appended V-nitrides,  $A^+[V^VN(OH)_3]^-$ ; the best-fit linear regression is shown.

creates more favorable conditions for methane activation. The  $Cs^+$  salt, interestingly, does not follow the trend in charges, Table 2, as well as the trend in activation energy calculations, Table 1, which may be due to the difficulties reported in modeling cesium compounds with effective core potential methods [20].

#### b. Electrostatic Effects of Alkali Metal Ions

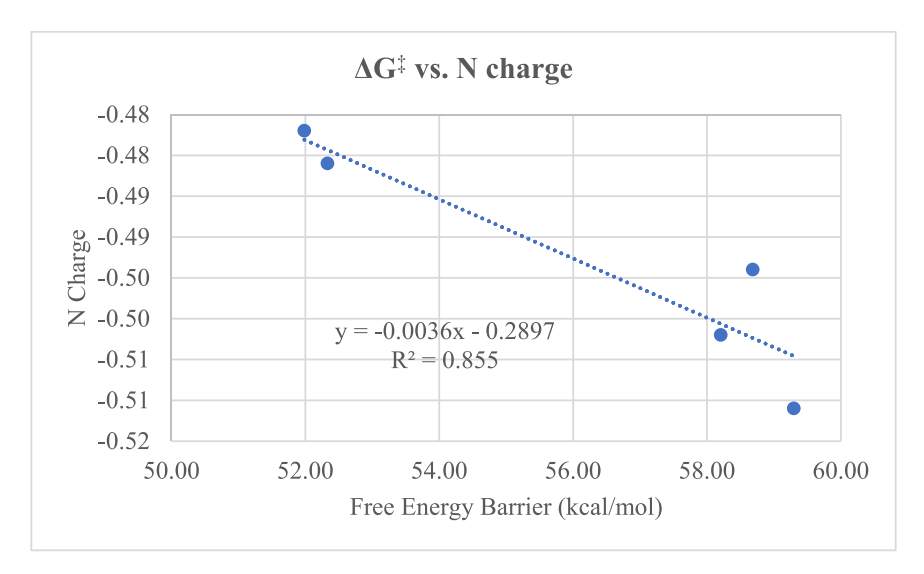


**Fig. 5.** Charge of nitride nitrogen (in  $e^-$ , as determined from a Mulliken population analysis) – y-axis – in an A<sup>+</sup>[V<sup>V</sup>N(OH)<sub>3</sub>]<sup>-</sup> complex versus the computed methane activation barrier (kcal/mol) – x-axis; linear regression fit is shown. Linear correlations with vanadium and alkali metal atomic charges were much weaker.

**Table 2** Mulliken atomic charges (in  $e^-$ ) of vanadium, nitride nitrogen, and alkali metal for reactant complexes and calculated methane activation energies (in kcal/mol) for methane 1,2-C—H addition to the V-nitride triple bond of  $A^+$ [VN(OH) $_3$ ] $^-$ .

A <sup>+</sup> metal	ΔG <sup>‡</sup> (kcal/mol)	V charge (e <sup>-</sup> )	N charge (e <sup>-</sup> )	A <sup>+</sup> metal charge (e <sup>-</sup> )
Li <sup>+</sup>	51.99	0.97	-0.48	0.73
Na <sup>+</sup>	52.33	0.94	-0.48	0.83
$K^+$	58.21	0.95	-0.50	0.84
$Rb^+$	59.30	0.98	-0.51	0.84
Cs <sup>+</sup>	58.69	0.94	-0.49	0.87

#### 3.4. Continuum solvent simulations

The effect of electrostatics upon methane activation was also investigated by modeling continuum solvents of varying polarity [18]:

benzene, THF (tetrahydrofuran), acetone, acetonitrile, and water (listed from least polar to most polar). Note that while stationary points were re-optimized for each continuum solvent, changes in geometries were minimal among the solvents investigated. Intriguingly, the gas phase reaction yielded the lowest calculated activation energy barrier. Although there are unusual "bumps" in the plots, in general as the polarity of the solvent increases, so do methane activation barriers (Fig. 6). The present results follow those observed for methane activation in the presence of outer sphere nucleophiles [7], i.e., a less polar environment was the most favorable vis-à-vis methane activation. Presumably, this is a manifestation of reduced screening of the electrostatic interaction by the medium between the cation and the active site atoms.

We only simulated anionic vanadium nitride anion (alkali metal absent) in polar solvents acetonitrile and water (*vide infra*) to reduce any artefacts arising from comparison of neutral and anionic entities in the gas phase. These calculations show that alkali metal ion appended systems, particularly for the lightest s-block cations, have significantly

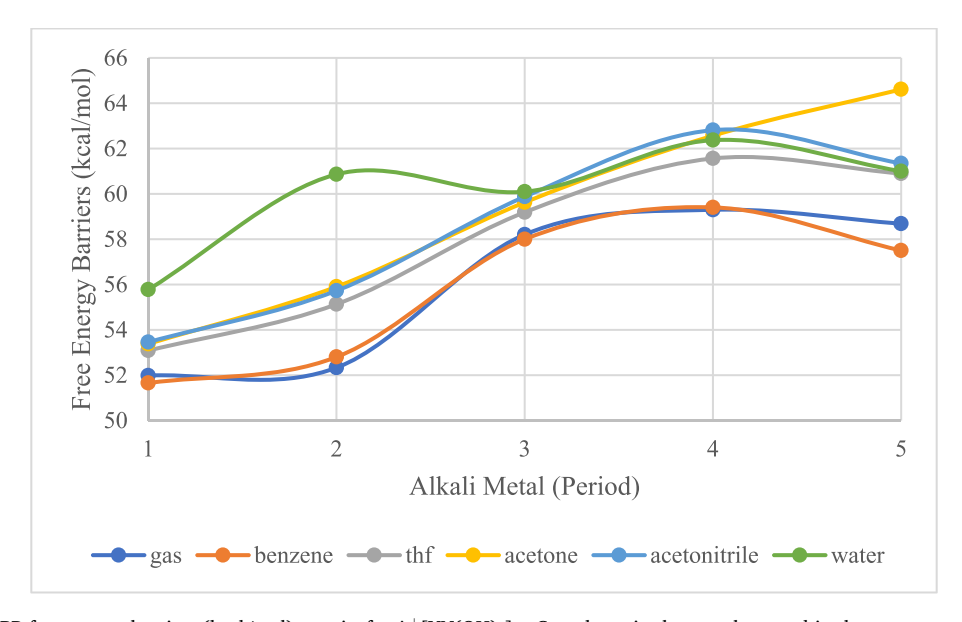


Fig. 6. B3LYP/def2-TZVPP free energy barriers (kcal/mol), y-axis, for  $A^+[VN(OH)_3]^-$ . Complexes in the gas phase and in the presence of SMD continuum solvent models (benzene, THF, acetone, acetonitrile, and water).  $1 = Li^+$  salt,  $2 = Na^+$  salt,  $3 = K^+$  salt,  $4 = Rb^+$  salt,  $5 = Cs^+$  salt.

lower energy methane activation barriers versus the corresponding anionic nitride complex. For example, in SMD-water, the  $\Delta G^{\ddagger}$  for methane activation by  $A^+[V(N)(OH)_3]$  range from  $\sim\!55.8$  (Li $^+$ ) to 62.4 (Cs $^+$ ) kcal/mol, Fig. 6, as compared to a free energy barrier of 67.0 kcal/mol for the anionic nitride complex. This indicates a  $\Delta\Delta G^{\ddagger}$  from alkali metal ion ligation of up to 11 kcal/mol! For SMD-acetonitrile, the computed  $\Delta\Delta G^{\ddagger}$  is as large as 12 kcal/mol in favor of the alkali metal salts. As before, smaller alkali metal ions yield lower methane activation barriers. For the Li $^+$  salt,  $\Delta G^{\ddagger}=53.5$  kcal/mol, as compared to  $\Delta G^{\ddagger}=65.8$  kcal/mol for the anion.

#### 4. Summary and conclusions

The research presented here models different alkali metal ions in the outer coordination sphere of model methane activating  $d^0$ -nitride complexes. The results suggest that electrostatic effects have the potential to significantly decrease methane activation barriers. Furthermore, lighter metal alkali metal cations in the outer coordination sphere yield lower methane activation barriers, with the lowest barrier being computed for the Li $^+$  salt. Additionally, barriers are reduced significantly,  $\Delta\Delta G^{\ddagger}>10\,$  kcal/mol, when comparing the anionic nitride complex to the Li $^+$  ion salts. Via variation of continuum solvent effects, this research demonstrates that  $A^+[VN(OH)_3]^-$  in gas phase reactions yielded the lowest activation energy barriers, suggesting that electrostatic effects are likely to be enhanced in the low polarity, hydrophobic solvents typically used for inorganic and organometallic complexes capable of methane activation.

#### CRediT authorship contribution statement

**Sarah Ann Teaw:** Data curation, Formal analysis, Investigation, Software, Writing – original draft, Writing – review & editing. **Thomas R. Cundari:** Conceptualization, Supervision, Writing – review & editing.

### Declaration of competing interest

The authors declare that they have no known competing financial interests or personal relationships that could have appeared to influence the work reported in this paper.

#### Data availability

Data will be made available on request.

#### Acknowledgements

This work was supported by the U.S. National Science Foundation under grant CHE-1953547, which is gratefully acknowledged. Additional NSF support for the UNT Chemistry HPC cluster via grants CHE-

1531468 and OAC-2117247 is also gratefully acknowledged.

#### References

- [1] S. Solomon, D. Qin, M. Manning, Z. Chen, M. Marquis, K.B. Averyt, M. Tignor, H. L. Miller, Contribution of Working Group I to the Fourth Assessment Report of the Intergovernmental Panel on Climate Change, Cambridge University Press, 2007.
- [2] G.A. Olah, Electrophilic methane conversion, Acc. Chem. Res. 20 (1987) 422-428.
- [3] P.T. Wolczanski, Activation of carbon-hydrogen bonds via 1,2-RH-addition/-elimination to early transition metal imides, Organometallics 37 (2018) 505–516.
- [4] Z. Sun, O.A. Hull, T.R. Cundari, Computational study of methane C-H activation by diiminopyridine nitride/nitridyl complexes of 3d transition metals and main-group elements, Inorg. Chem. 57 (2018) 6807–6815.
- [5] D.C. Alamo, T.R. Cundari, DFT and TDDFT study of the reaction pathway for double intramolecular C-H activation and functionalization by Iron, cobalt, and nickel-nitridyl complexes, Inorg. Chem. 60 (2021) 12299–12308.
- [6] R. Thompson, B.L. Tran, S. Ghosh, C.H. Chen, M. Pink, X. Gao, P.J. Carroll, M. H. Baik, D.J. Mindiola, Addition of Si-H and B-H bonds and redox reactivity involving low-coordinate nitride-vanadium complexes, Inorg. Chem. 54 (2015) 3068–3077.
- [7] M.E. Anderson, B. Braïda, P.C. Hiberty, T.R. Cundari, Revealing a decisive role for secondary coordination sphere nucleophiles on methane activation, J. Am. Chem. Soc. 142 (2020) 3125–3313.
- [8] T.R. Cundari, B.P. Jacobs, S.N. MacMillan, P.T. Wolczanski, Dispersion forces play a role in (Me2IPr)Fe(=NAd)R2 (Ad = adamantyl; R = neoPe, 1-nor) insertions and Fe-R bond dissociation enthalpies (BDEs), Dalton Trans. 2018 (47) (2018) 6025-6030.
- [9] N.G. Léonard, T. Chantarojsiri, J.W. Ziller, J.Y. Yang, Cationic effects on the net hydrogen atom bond dissociation free energy of high-valent manganese imido complexes. J. Am. Chem. Soc. 144 (2022) 1503–1508.
- [10] W.S. Alharbi, T.R. Cundari, Mapping the basicity of selected 3d and 4d metal nitrides: A DFT study, Inorg. Chem. 61 (2022) 19049–19057.
- [11] J.M. Smith, Reactive transition metal nitride complexes, Prog. Inorg. Chem. 58 (2014) 417–470.
- [12] M.V. Kirillova, M.L. Kuznetsov, P.M. Reis, J.A.L. da Silva, J.J.R. Frausto da Silva, A. J.L. Pombeiro, Direct and remarkably efficient conversion of methane to acetic acid catalyzed by amavadine and related vanadium complexes. A synthetic and a theoretical DFT mechanistic study, J. Am. Chem. Soc. 129 (2007) 10531–10545.
- [13] J. Deng, S.C. Lin, J.T. Fuller III, B. Zandkarimi, H.M. Chen, A.N. Alexandrova, C. Liu, Electrocatalytic methane functionalization with d<sup>0</sup> early transition metals under ambient conditions, Angew. Chem. 133 (2021) 26834–26842.
- [14] J. Deng, S.C. Lin, J. Fuller III, J.A. Iñiguez, D. Xiang, D. Yang, G. Chan, H.M. Chen, A.N. Alexandrova, C. Liu, Ambient methane functionalization initiated by electrochemical oxidation of a vanadium (V)-oxo dimer, Nature Comm. 11 (2020) 3686
- [15] A. Najafian, T.R. Cundari, Effect of appended s-block metal ion crown ethers on redox properties and catalytic activity of Mn-nitride Schiff base complexes: methane activation, Inorg. Chem. 58 (2019) 12254–12263.
- [16] B.M. Prince, T.R. Cundari, Methane C-H bond activation by "naked" alkali metal imidyl and alkaline earth metal imide complexes. The role of ligand spin and nucleophilicity, J. Phys. Chem. A 117 (2013) 9245–9251.
- [17] M.J. Frisch, G.W. Trucks, H.B. Schlegel, G.E. Scuseria, M.A. Robb, J.R. Cheeseman, G. Scalmani, V. Barone, G.A. Petersson, H. Nakatsuji, et al. *Gaussian 16, Revision* A.03; Gaussian, Inc.: Wallingford, CT, (2016).
- [18] A.V. Marenich, C.J. Cramer, D.G. Truhlar, Universal solvation model based on solute electron density and on a continuum model of the solvent defined by the bulk dielectric constant and atomic surface tensions, J. Phys. Chem. B 113 (2009) 6378–6396.
- [19] G.S. Hammond, A correlation of reaction rates, J. Am. Chem. Soc. 77 (1955) 334–338.
- [20] M. Krauss, W.J. Stevens, Effective core potentials and accurate energy curves for Cs<sub>2</sub> and other alkali diatomics, J. Chem. Phys. 93 (1990) 4236–4242.